Light harvesting with non covalent carbon nanotube / porphyrin compounds.

Cyrielle Roquelet, Benjamin Langlois, Fabien Vialla, Damien Garrot, Jean-sébastien Lauret, Christophe Voisin

Light harvesting with non covalent carbon nanotube / porphyrin compounds.

C. Roquelet[a], B. Langlois[b], F. Vialla[b], D. Garrot[a,b], J.S. Lauret[a], C. Voisin[b,*]

[a] *Laboratoire de Photonique Quantique et Moléculaire, Institut d'Alembert, CNRS, ENS Cachan, 94235 Cachan, France*
[b] *Laboratoire Pierre Aigrain, École Normale Supérieure, CNRS UMR 8551, UPMC, Université Paris Diderot, 24 rue Lhomond, 75005 Paris, France*

Abstract

We present recent developments in the synthesis and in the functional study of non covalently bound porphyrin/carbon nanotube compounds. The issue of the chemical stability of non covalent compounds is tackled by means of micelle assisted chemistry. The non covalent functionalization allows to preserve the electronic integrity of the nanotubes that display bright NIR luminescence. In the same time, the coupling between the subunits is very strong and leads to efficient energy transfer and PL quenching of the chromophore. This transfer occurs on a subpicosecond time-scale and leads to a near 100% efficiency. It allows to uniformly excite a whole set of chiral species with a single wavelength excitation. Insight into the transfer mechanism is gained by means of transient absorption spectroscopy.

Keywords: Carbon nanotubes; Porphyrins; Energy transfer; Transient spectroscopy; Photoluminescence; Micelle swelling.

1. Introduction

Single Wall Carbon Nanotubes (SWNTs) are famous for their many fascinating physical properties opening the way to promising applications. In the same time, they appear as unique prototypes of quasi one dimensional objects allowing unprecedented testing of basic physical effects. However, it appeared rapidly that the structure of nanotubes with all atoms at the surface, leads to strong interactions with the environment that can possibly induce a drastic alteration of their properties. For instance, the interaction of nanotubes with a substrate can lead to a full quenching of their luminescence [1, 2] or to an important degradation of their electronic transport properties [3, 4]. Several strategies were proposed to overcome these effects such as the encapsulation of nanotubes in micelles of surfactant [5, 6] or in various polymers [7], or such as the use of suspended nanotubes [1, 8]. On the other hand, the ability of SWNTs to interact with their environment can be used favorably as a way to create new functional materials. This is the field of functionalized nanotubes, where the general philosophy is to put together organic molecules and carbon nanotubes in order to combine their specific properties and possibly create new ones due to the interaction between the two species. The approach turned out to be highly valuable in many fields including opto-electronics, chemistry or biology [9, 10]. In this quest, a general compromise has to be found between the robustness of the compound and the preservation of the properties of the tube. In fact, covalent functionalization leads to the most stable compounds but also significantly alters the transport and optical properties of the nanotubes [11, 12]. In contrast, non covalent compounds allow to preserve these intrinsic properties, which is highly valuable for many applications, but at the cost of the chemical stability.

In this paper, we report on a new approach based on micelle assisted chemistry that allows to obtain non covalent compounds that show at the same time a remarkable stability and an excellent coupling between the molecule and the nanotube. This coupling between the chromophore and the nanotube gives rise to an extremely efficient energy transfer that allows to enhance considerably the effective absorption cross section of the nanotube in the visible range, while preserving its emitting properties in the near infrared (NIR) range. This kind of compounds may be of interest for long term applications such as light harvesting and bio labeling. In the latter case for instance, the NIR emission of nanotubes could be profitable since it matches the window of relative transparency of biological tissues. Therefore, the preservation of the luminescence properties of nanotubes is essential, while the molecules could be used to bind the compound with specific targets allowing functional imaging of biological tissues. Regarding photo-voltaic applications, carbon nanotubes are known to be good electron acceptors and allow to separate the photo generated electron-hole pairs when associated to various organic materials and polymers [13, 14, 15, 16, 10, 17]. In this case, the use of non covalent functionalization allows to preserve the electronic mobility of the nanotubes and therefore allows to reduce the losses in the device.

Although these investigations are motivated by possible long term applications, we focus in this paper on a basic investigation of the microscopic mechanisms leading to the efficient electronic coupling in non covalent compounds. In this perspective, we focus on the properties of a non-covalently bound porphyrin/nanotube compound (H_2TPP@SWNT) showing efficient energy transfer, which allows a full optical investigation of the coupling including time-resolved studies. These compounds are made of a layer of free base tetraphenyl porphyrin molecules (H_2TPP) π-stacked on the wall of the nanotubes (Co-

*Corresponding author : christophe.voisin@lpa.ens.fr

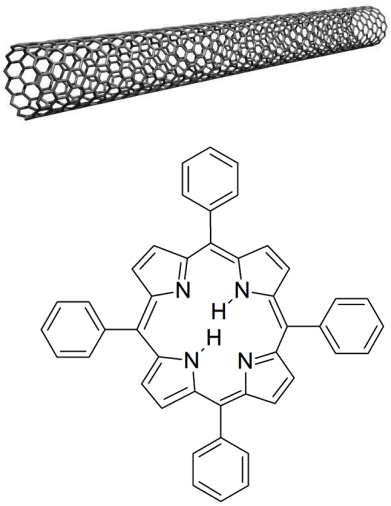

Figure 1: (color online) Schematic representation of a SWNT and of the H_2TPP molecule.

MoCat SG65) (Fig. 1). Porphyrin is a major building block in bio-chemistry. It stands for the backbone in chlorophylls and hemoglobin molecules. It is also well known for its photophysical properties especially in the photosynthesis cycle and was previously used as sensitizer for organic photovoltaic cells [18].

We first review the fabrication process and the structural characterization of the compound. Then, we propose a set of methods to evaluate the efficiency of the coupling between the chromophore and the nanotube including studies at the single nano-compound scale, that show the statistical distribution of the transfer yield and its correlations to other spectroscopic features. Finally, the dynamics of the transfer is investigated on a sub-picosecond time-scale and insight is given into the microscopic mechanism driving the energy transfer.

2. Synthesis and structural investigation

SWNTs are known to show strong π interactions between each other and to form strongly bound bundles. In these bundles, the electronic coupling between the tubes leads to efficient energy transfer between semi-conducting nanotubes [19, 20]. For larger bundles where the presence of metallic nanotubes is very likely, this coupling eventually leads to an extremely strong quenching of the luminescence of semi-conducting nanotubes [21]. Therefore, in order to functionalize carbon nanotubes and benefit from their intrinsic properties, it is necessary to first split the bundles and obtain individualized nanotubes. A well known and wide spread strategy is the use of surfactants that leads to the creation of micelles containing individualized SWNTs [5, 6]. In a first attempt to reach non covalent functionalization of SWNTs with porphyrin molecules, we tried to use hydrophilic porphyrins (TPPS) as a surfactant [22]. Other groups used similar approaches or tried for instance to substitute the surfactant by an amphiphilic chromophore in a micelle suspension of carbon nanotubes [23]. These approaches are interesting because they show unambiguously that the interaction between the porphyrin and the nanotubes through the "π stacking interaction" can be strong enough to allow the dissolution of carbon nanotubes in water. In addition, the first indications for a strong coupling and energy transfer was demonstrated in this system [22]. However, the stability of the suspensions turned out to be poor with flocculation within a couple of days.

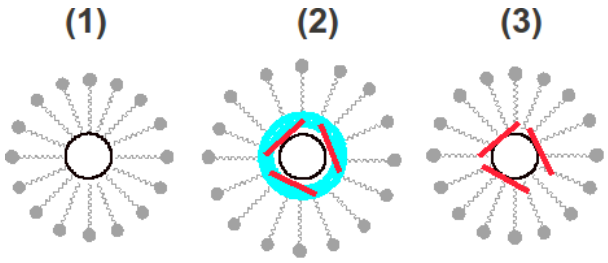

Figure 2: (color online) Sketch of the micelle swelling method. An organic micro-environment is created around the nanotube by swelling the micelle with an organic solvent that brings the chromophore. After evaporation of the solvent a non-covalently functionalized nanotube remains in the core of the micelle.

The new approach that we developed is based on the idea that the stability of the nanotube/porphyrin compounds could be enhanced using hydrophobic porphyrins inserted in the core of regular micelles (sodium cholate) together with the nanotubes. However, it is not straightforward to drive the hydrophobic molecule through water into the micelle. The micelle swelling method allowed us to do so [24]. In this method, hydrophobic porphyrins are first dissolved in an organic solvent such as dichloro-methane (DCM) and mixed to a regular water micellar suspension of carbon nanotubes by means of ultrasonic stirring. The fact that an organic solvent can penetrate the core of micelles with this method was demonstrated independently by Wang et al. [25] and later applied successfully to other compounds [26]. The scheme of the method is depicted in Fig. 2. As demonstrated below, the organic solvent serves as a vector to take the hydrophobic molecules to the core of the micelle.

Optical absorption spectroscopy is a powerful tool to monitor the functionalization process. Actually, the presence of porphyrin molecules on the wall of the nanotubes induces several clear spectroscopic features (Fig. 3). First the nanotube transitions show a sizable redshift which is mainly due to the screening of the Coulomb interactions in the nanotubes by the adsorbed molecules [2]. In addition, the appearance of a large absorption band in the blue part of the visible spectrum is the signature of the presence of porphyrin molecules in the micelles. This band corresponds to the Soret band of the porphyrin, but in the case of adsorbed molecules, its position is slightly red shifted because of conformational changes in the molecule [22]. Therefore a split Soret band is observed with one peak at 420 nm corresponding to porphyrin molecules alone in a micelle and another peak at 440 nm corresponding to the molecules adsorbed on the nanotube wall. Therefore, the intensity and the ratio of these peaks allow to monitor the amount of H_2TPP incorporated in the suspension and the amount of H_2TPP adsorbed on the nanotube wall. In addition, the shift of

the nanotube bands is a probe of the nanotube coverage.

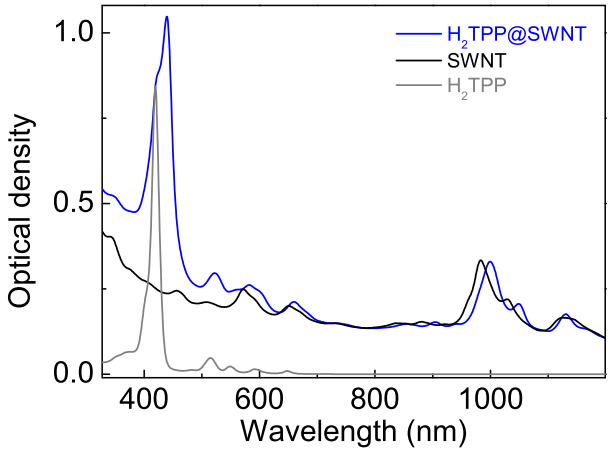

Figure 3: (color online) Absorption spectrum of a micellar suspension of CoMoCat nanotubes (black line), a micellar suspension of H_2TPP (gray line) and a suspension of functionalized nanotubes (blue line).

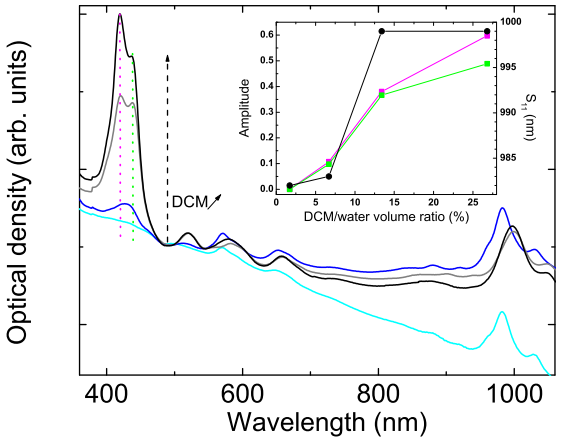

Figure 4: (color online) Absorption spectra of H_2TPP/SWNT suspensions obtained for various DCM/water volume ratio : 2% (light blue), 7% (blue), 13% (gray) and 27 % (black). The quantity of H_2TPP is constant (0.14 μmol) and the water volume is 2.5 mL. The spectra were vertically translated in order to compensate for the background scattering at 490 nm. Inset : Maximum value of the absorption bands of free H_2TPP at 420 nm (pink), of stacked H_2TPP at 438 nm (green) and position of the S_{11} transition of (6,5) SWNTs (black, right scale) as a function of the DCM/water volume ratio. (Figure taken from Ref.[24]).

We first checked the role of the organic solvent in the functionalization process by varying the ratio between the DCM and water volumes, while keeping the amount of H_2TPP molecules and of nanotubes constant (Fig. 4). For a DCM/water ratio of 5% or less the functionalization is negligible even after a long sonication time. In contrast, increasing this ratio up to 25% leads to an enhanced functionalization. Larger amounts of DCM do not lead to a better functionalization yield. This clearly brings evidence for the role of the organic solvent as a vector for the H_2TPP molecules.

We also checked the role of the stoichiometry and varied the total amount of H_2TPP molecules brought in the DCM solution (Fig. 5). Again, we found that all indicators (SWNTs shifts, shift of the Soret band) first show an increasing functionalization when rising up the H_2TPP amount and then a plateau for 0.15 μmol and above. We attribute this plateau to the completion of the first layer of H_2TPP around the nanotube wall. (Additional evidence for this result is given in Sec.3.) This assertion is qualitatively accounted for by a rough estimate of the number of H_2TPP molecules that the surface of the SWNTs can accommodate. Actually, we find that the optimal amount of H_2TPP molecules (0.15 μmol) can cover an area equivalent to 0.04 mg of SWNTs, whereas the SWNTs suspension was initially prepared with 0.15 mg. These values are consistent since a large amount of SWNTs are lost in the preparation of individualized nanotubes (centrifugation step). Above this threshold, the amplitude of the peak at 420 nm keeps rising, showing that additional H_2TPP molecules are encased in individual micelles rather than on the wall of the nanotubes. Note however that for much larger concentrations of porphyrin (50 times larger), we can reach another regime where several layers of porphyrins are wrapped around the nanotube [27].

The data presented here above were collected for samples made from CoMoCat nanotubes (SG65), but similar results

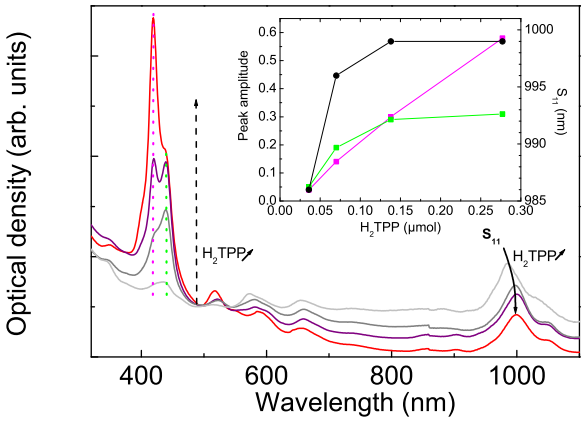

Figure 5: (color online) Absorption spectra of H_2TPP@SWNT micellar suspensions for various amounts of H_2TPP (the water volume is 2.5 mL) : 0.04 μmol (light gray), 0.07 μmol (gray), 0.14 μmol (purple), 0.28 μmol (red). The DCM/water volume ratio is kept constant (34%). The spectra were vertically translated in order to compensate for the background scattering at 490 nm. Inset : Maximum value of the absorption bands of free H_2TPP at 420 nm (pink), of stacked H_2TPP at 438 nm (green) and position of the S_{11} transition of (6,5) SWNTs (black, right scale) as a function of the added H_2TPP amount. (Figure taken from Ref.[24]).

were obtained for HiPCO or laser ablation nanotubes. In addition, this functionalization method can be extended to other molecules such as metalled porphyrins or phthalocyanines (see Supporting Information).

Finally, note that the compounds show an excellent stability over time (see Supporting Information). We were also able to fabricate solid thin films of the compounds that display very similar optical properties as compared to the suspensions (see Supporting Information).

3. Energy transfer

Although these compounds are non-covalently bound, they display an important coupling between the chromophore and the nanotube, which allows to combine their properties and design new functionalities. In the particular case of H_2TPP@SWNTs compounds, this coupling leads to an efficient energy transfer from the chromophore to the nanotube. Practically, the near NIR luminescence of the nanotubes is strongly enhanced when the excitation wavelength matches the absorption bands of the chromophore. This energy transfer is observed both in suspensions and in thin solid films (see Supporting Information).

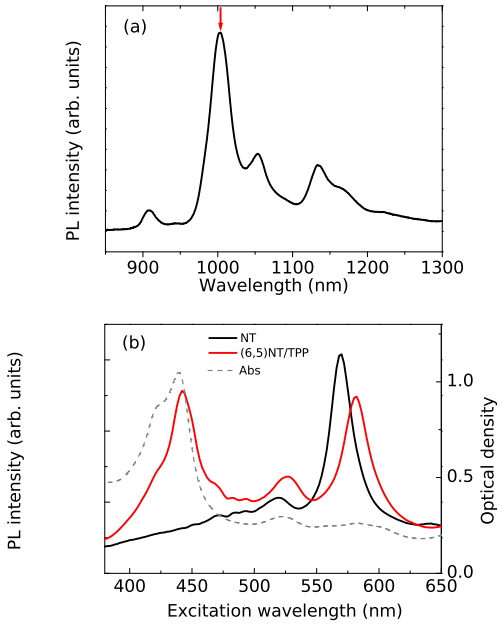

Figure 6: (color online) (a) PL spectrum of a micellar H_2TPP@SWNT suspension excited at 532 nm. (b) PLE spectrum of a SWNT suspension detected at 984 nm (black line) and of a H_2TPP@SWNT suspension detected at 1007 nm (red line, (6,5) species, vertical arrow in (a)). Absorption spectrum of the H_2TPP@SWNT suspension (dashed line).

In the visible range, the photoluminescence excitation spectra (PLE) of each NIR PL line shows two major resonances (see Fig. 6). One of them always lies at 438 nm, which corresponds to the Soret band of H_2TPP stacked on nanotubes. The fact that this resonance matches only the redshifted peak of the Soret band confirms that we have two H_2TPP species in the sample : the H_2TPP molecules stacked on the nanotubes that are selectively excited at 438 nm and the free H_2TPP encased in micelles showing a Soret band at 420 nm.

The second resonance in the PLE spectrum of the fonctionnalized nanotubes shows up at 570 nm for (6,5) nanotubes but at other wavelenths for other chiral species (not shown, see [28]). This resonance corresponds to the direct excitation of the nanotubes on their S_{22} resonance.

The striking feature in the PLE spectrum of the compound (Fig. 6) is that the intrinsic S_{22} resonance and the energy transfer resonance have roughly the same magnitude. This allows a first estimate of the quantum efficiency η of the energy transfer [29]. This equal intensity of the two resonances means that the flux of photons emitted by the nanotubes is the same when the compound is excited directly through the S_{22} resonance of the nanotube or when it is excited through the Soret absorption of the H_2TPP followed by energy transfer to the nanotube. This means that the intrinsic S_{22} absorption is roughly equal to the global absorption of all the H_2TPP molecules stacked on the nanotube multiplicated by the transfer quantum yield ($\sigma_{S22} \simeq \eta N \sigma_{H_2TPP}$). The number of molecules N is evaluated from the geometrical parameters of the nanotube and of the molecule assuming a full coverage by one single layer of H_2TPP molecules as inferred from the synthesis monitoring. Values for the absorption coefficients are taken from the litterature ($\sigma_{S_{22}} = 1.1 \pm 0.1\text{x}10^{-12}$ cm^2/μm, $\sigma_{H_2TPP} = 7\text{x}10^{-16}$cm^2) [30, 31]. We deduce that the transfer yield is very high, of the order of 95% [29].

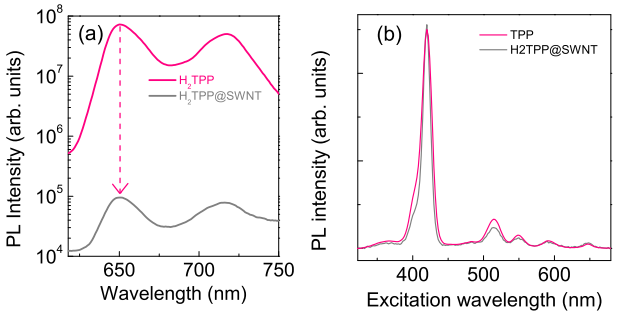

Figure 7: (color online) (a) PL spectrum of free H_2TPP encased in micelles for an excitation wavelength of 420 nm (red line). Visible PL spectrum of H_2TPP@SWNT (excitation wavelength 438 nm, grey line). (b) Normalized PLE spectra (detection at 720 nm) of the H_2TPP sample (red line) and the H_2TPP@SWNT sample (grey line). (Figure inspired from Ref. [29]).

As expected, this energy transfer is associated with a strong quenching of the luminescence of the donor. Free H_2TPP gives rise to bright PL lines at 650 nm and 720 nm associated with vibronic transitions from the Q levels. In functionalized nanotubes, this luminescence is reduced by at least 3 orders of magnitude (see Fig. 7). Actually, the residual PL measured in functionalized nanotubes does not arise from the compounds them-

selves, but rather from the residual free H_2TPP encased in micelles as shown by the PLE spectrum centered at 420 nm, rather than 438 nm as would be expected for stacked porphyrins (see Fig. 7). Although the quenching cannot be precisely measured due to this residual signal from free H_2TPP, it nevertheless allows us to draw another independent estimate of the transfer quantum yield. Assuming that the quenching is mainly due to the transfer of the excitation from the H_2TPP to the nanotube, we write : $\eta = 1 - I^{PL}_{H_2TPP@SWNT}/I^{PL}_{H_2TPP} \geq 99.9\%$.

PLE measurements also allow to enlighten the relationship between the coverage of the nanotube surface and the energy transfer. For this purpose, we synthesized a suspension with a reduced amount of H_2TPP. We performed thorough PLE measurements by varying the detection wavelength between 990 nm and 1010 nm, which corresponds to the span of the S_{11} transition in (6,5) nanotubes. The results are shown in Fig. 8.

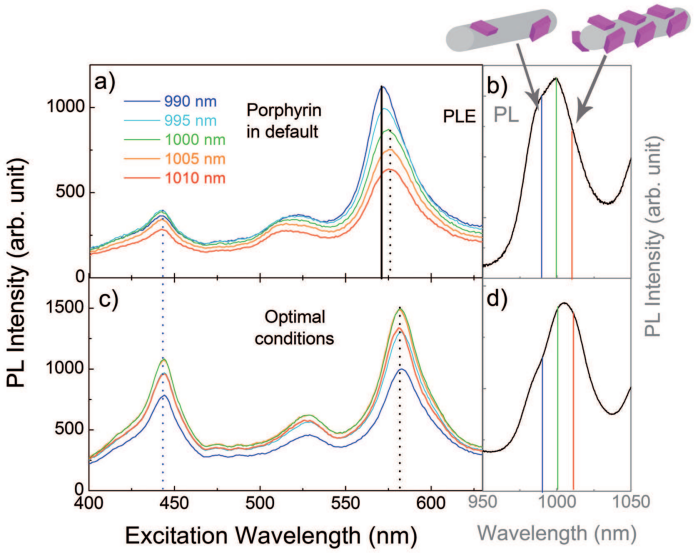

Figure 8: (color online) PLE spectra for various detection wavelengths spanning the inhomogeneous S_{11} line of (6,5) nanotubes for a suspension with a reduced H_2TPP amount (0.05 μmol) (a) and for a suspension with optimal H_2TPP amount (0.14μmol) (c). The detection window is 10 nm wide. PL spectra of the default suspension (b) and optimal suspension (d).

This set of measurements actually allows to probe the inhomogeneous broadening of the S_{11} line. In accordance with the results shown in Fig. 5, the largest redshifts correspond to a subset of nanotubes with relatively high coverage, whereas the blue wing of the line corresponds to almost bare nanotubes. The S_{22} resonance shows a increasing red shift for increasing detection wavelength. The positive correlation between the shifts of S_{11} and S_{22} is consistent with a H_2TPP induced dielectric screening of excitons in carbon nanotubes [2, 32]. In contrast, for all subsets of nanotubes, the energy transfer resonance shows up at the same wavelength (438 nm). This means that the shift of the Soret band in stacked H_2TPP is not related to the H_2TPP concentration and therefore to any aggregate formation, but is only due the interaction between each molecule and the nanotube.

In addition, it is interesting to note that the amplitude of the energy transfer resonance is not simply proportional to the amplitude of the S_{22} resonance (and thus to the population of the nanotube subset selected by the detection wavelength). The ratio R between the the energy transfer resonance and intrinsic S_{22} resonance is plotted as a function of the detection wavelength in Fig.9. The larger the redshift of the excitonic line, the larger the transfer ratio. Once more, this is consistent with the picture of a subset of highly covered nanotubes showing a large redshift and a high transfer ratio (since many porphyrin molecules are involved in the transfer). In contrast, the blue wing of the inhomogeneous excitonic transition corresponds to a low coverage of the nanotube surface and therefore to a low transfer ratio. Note that this low transfer ratio is not related to a lower quantum transfer efficiency but simply reflects the lower number of chromophores involved in the transfer. Interestingly, for an optimal H_2TPP concentration and above, the inhomogeneous broadening of the excitonic line vanishes and gives rise to identical S_{22} energies and transfer ratios wathever the detection wavelength (Fig. 8 (c) and (d) and Fig. 9). This shows that we reach the completion of the first layer of porphyrin on the wall of the nanotube. The creation of a second layer is unlikely since the transfer yield and the line at 440 nm do not rise further for larger porphyrin concentration. We believe that the excess H_2TPP molecules are rather trapped in empty micelles (the surfactant is in large excess). Actually if the excess porphyrin molecules were inserted in the micelles containing the completed H_2TPP@SWNT compounds to form a second layer, this would give rise to a shifted absorption feature since J (resp. H) aggregates of H_2TPP are known to display large red (resp. blue) shifts [33]. In contrast, the absorption and emission wavelengths of this excess porphyrin matches the ones of free porphyrin in micelles. In total, we believe that the H_2TPP@SWNT compound obtained in optimal conditions consist in one and one only completed layer of porphyrin molecules wrapped on the wall of the nanotube.

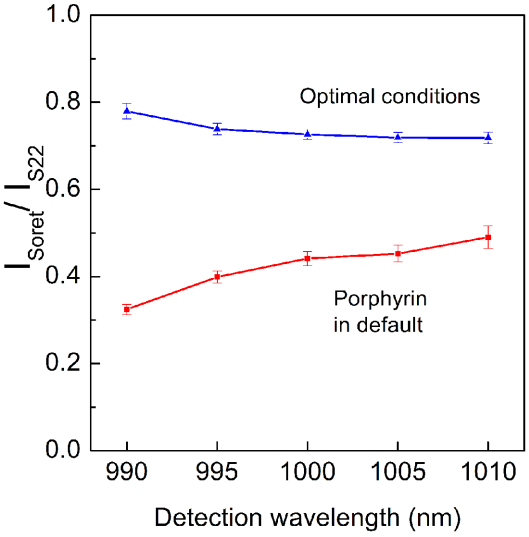

Figure 9: (color online) Ratio of the PL intensity obtained for an excitation wavelength on the Soret band (440 nm) and on the S_{22} transition as a function of the detection wavelength for the default suspension (red line) and the optimal suspension (blue line).

Finally, we performed the PLE investigation of the energy transfer at low temperature on a thin film of H_2TPP@SWNTs encased in micelles (see Fig. 10). The main result is that the transfer yield does not depend drastically on the temperature. At most a decrease of about 25% is observed when cooling the sample down to 10 K. However, this reduction of the transfer ratio lies within our error bar due to normalization issues in the setup used for this measurement. This weak temperature dependence rules out that the transfer mechanism is mainly assisted by phonons, except if very low energy modes are specifically involved. In contrast, the persitance of an efficient energy transfer at low temperature is rather in line with a pure electronic process, as discussed in section 6.

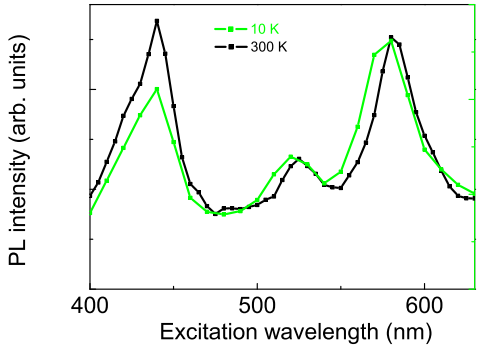

Figure 10: (color online) PLE spectra of (6,5) nanotubes in a thin film of H_2TPP@SWNTs (detection : 1005 nm) at room temperature (black line) and 10 K (green line).

4. Investigation of the energy transfer at the single nanocompound scale

In contrast to ensemble measurements that only allow to measure the average energy transfer yield, single object spectroscopy allows to gain insight into the nanoscale statistical distribution of this transfer yield (see Methods). In order to assess this point quantitatively, we use the transfer efficiency R (ratio between the PL intensity of the nanotubes excited on the Soret resonance and the PL intensity of the nanotubes excited on the intrinsic S_{22} resonance). Note that this ratio does not reflect directly the transfer quantum yield [29] because the absorption cross-section and the internal energy conversion may vary with the chiral species [34, 35]. In fact, this ratio R may even be larger than 1. However, the fluctuations of this ratio for different single compounds based on the same chiral species fairly reflect the statistical transfer yield variations. In fact, being a ratio of two PL intensities from the same (S_{11}) transition in the very same nano object, this ratio does not depend on presence of local quenching sites or mechanisms. Therefore, it only reflects the local fluctuations regarding the energy transfer process.

We plot in Fig. 11 the transfer efficiency R as a function of the spectral shift of the S_{11} transition with respect to the average value measured for bare nanotubes. A general trend is that the higher the spectral shift, the larger the transfer efficiency.

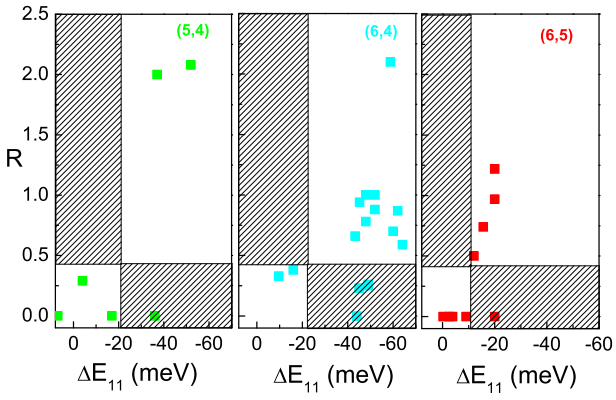

Figure 11: (color online) Transfer efficiency versus spectral shift of the S_{11} transition (with respect to the bare nanotube case) for three chiral species (data were recorded at 10 K). The data are mainly distributed in the lower left and upper right frames of each plot, which shows that energy transfer and screening of the optical transition of the nanotube are correlated.

As can be seen from the figure, almost all points fall into two groups that correspond to the lower left and upper right frames : the former group shows low spectral shifts and low transfer efficiencies and the latter group shows large spectral shifts and high transfer efficiencies. The spectral shift of the transition is primarily assigned to the screening of nanotube's exciton by the surrounding porphyrin molecules [22, 24, 14]. In this respect, the correlation between the shift and the transfer efficiency simply reflects that the latter is closely related to the coupling strength between the porphyrin and the tubes. However, this coupling can vary from one tube to another either due to surface coverage fluctuations or due to variations in the average nanotube-porphyrin distance. We note however that a few compounds show a sizable spectral shift together with a very limited transfer efficiency. These compounds may be bare nanotubes screened by other surrounding species (surfactant, substrate) or being mechanically stressed [14, 2]. Note finally that this statistics does not necessarily reflect the composition of the suspensions since defunctionnalization or aggregation may occur during the deposition on the substrate.

5. Time-resolved investigation of the energy transfer

The demonstration of efficient energy transfer in non covalently bound porphyrin/ carbon nanotube compounds raises two important questions. The first one is why this energy transfer is so efficient and what is the time-scale associated with this transfer. The second one is related to the underlying mechanism and the electronic states involved in the transfer. Transient absorption spectroscopy is a very powerful tool to address these questions, since it allows to monitor the populations of all electronic states of the material upon excitation, together with their relaxation dynamics. We carried out such transient absorption measurements on H_2TPP@SWNTs samples by means of a broad band pump-probe setup (see Methods).

We first applied this technique to monitor the relaxation dynamics on the Soret band of H_2TPP. Fig. 12 shows the transient transmission dynamics for a pump and a probe in resonance with the Soret band in a micellar suspension of free H_2TPP and in a micellar suspension of H_2TPP@SWNT.

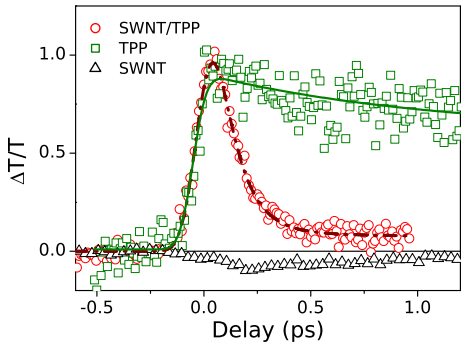

Figure 12: (color online) Normalized transient transmission dynamics measured in a degenerate configuration in resonance with the Soret band in free H_2TPP in micelles (green squares), in H_2TPP@SWNT in micelles (red dots). Same measurement at 438 nm in bare SWNTs in micelles (black triangles) which allows to check that the intrinsic signal from SWNTs is negligible at this wavelength (from Ref. [28]).

The transient transmission of free H_2TPP shows a relatively slow relaxation dynamics. This is the signature of a slow ground state recovery [36]. Whereas the population of the upper electronic state of the Soret transition (B state) relaxes down to Q states within a few tens of femtoseconds [36] (see Fig. 15), which is beyond our time resolution, the population stays for a long time on the Q_x band from which the PL signal arises (about 10 ns lifetime [36]) before relaxing to the ground state. In contrast, H_2TPP@SWNT shows an ultrafast recovery, meaning that the porphyrin ground state is repopulated within a few hundreds of femtoseconds. This is the consequence of the excitation energy transfer to the nanotube. Therefore, we can deduce that the typical time-scale of this energy transfer is of the order of a few hundreds of fs, much faster than the relaxation time of the Q bands of the porphyrins. This explains why the yield of the transfer is so high. We can actually assess this quantum yield from the time-resolved data and write $\eta \simeq 1 - \tau_{H_2TPP@SWNT}/\tau_{H_2TPP} \simeq 99.99\%$, which is consistent with our previous estimates (see Sec. 3). Note that the small plateau at longer delays is due to residual free H_2TPP. We checked that this plateau does increase when tuning the wavelength down to 420 nm.

Transient absorption spectroscopy allows to go a step further and to monitor the population buildup in SWNTs upon excitation of the compound on the Soret band of the porphyrin. For this measurement, we used a pump wavelength at 445 nm in resonance with the Soret band of H_2TPP@SWNTs and a broad NIR probe that allows to measure the bleaching of the S_{11} transitions of the different chiral species. The resulting transient spectra are presented in Fig. 13 for several pump-probe delays.

The transient differential transmission shows several positive peaks corresponding to the photo-bleaching of the S_{11} transitions of the different chiral species. The transient spectra and the linear absorption spectrum show striking similarities, which clearly indicates that the energy transfer is not chiral selective, at least for the set of chiral species probed in this spectral window. Therefore, functionalization of SWNTs with chromophores having a large absorption cross-section appears as a convenient way to excite efficiently and uniformly the whole set of chiral species of a sample. Finally, in line with the strong induced PL signal of the nanotubes, we do not see any signature of charged species.

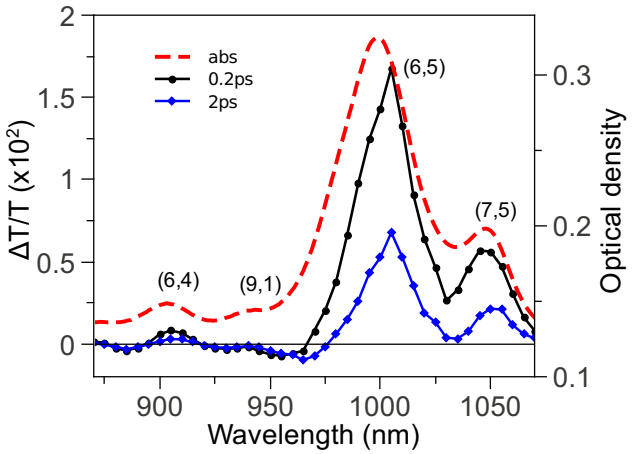

Figure 13: (color online) Transient absorption spectrum of H_2TPP@SWNT for a pump at 445 nm in resonance with the Soret band and a broadband probe in the NIR. The pump-probe delay is 0.2 ps (black dots) and 2 ps (blue squares). Right axis : linear absorption of the sample (dashed line). The majority chiral species is indicated in parenthesis for each line. (Figure inspired from Ref. [28]).

The dynamics of this S_{11} population build-up was studied by choosing a probe wavelength at 1005 nm in resonance with the (6,5) chiral species. Similar results were obtained for other chiral species (not shown). The transient change of transmission is compared to the one of bare SWNTs in Fig. 14. First, we note that the signal rise is almost instantaneous at the scale of our Instrumental Response Function (IRF), that is smaller than 300 fs. This is consistent with the measurements presented in Fig. 12 that show a decay of the TPP population of the order of 100 fs. The population therefore reaches the S_{11} excitonic levels almost immediately after being transfered to the nanotube and we can deduce that there is no population accumulation on any other intermediate electronic state. However, one cannot rule out that S_{22} excitonic levels may be involved in the transfer mechanism since they are known to have an extremely brief lifetime [21, 37]. The decay of the induced S_{11} population is very similar in functionalized and bare nanotube, although slightly faster in the former. This means that the attached molecules do not open significant additional non radiative channels, which is consistent with the large PL signal observed in these compounds as expected for non covalent functionalization. Finally, the raw data (non shown) indicate that the S_{11} bleaching measured in functionalized nanotubes is about 4 times larger than in bare nanotubes for identical pump

fluences. This increased signal amplitude is consistent with the 5-fold increased PL signal in the same conditions. It is difficult however to compare these signal levels with the respective absorption of both samples at the pump wavelength since the absorption in bare SWNT is non resonant at this wavelength and the contribution of the (6,5) species is therefore impossible to extract from the linear absorption spectrum.

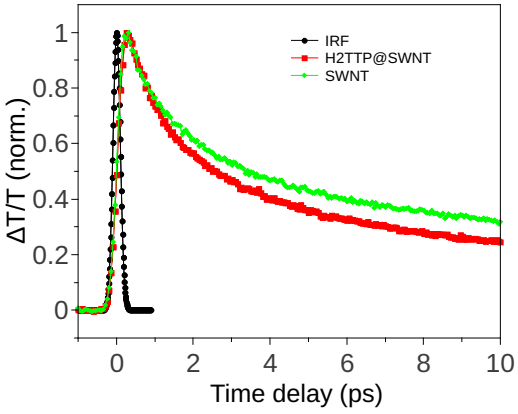

Figure 14: (color online) Normalized transient transmission dynamics for a pump wavelength of 445 nm and a probe in resonance with the S_{11} transition of (6,5) nanotubes : micellar suspension of H_2TPP@SWNT (red squares, probe at 1005 nm) and reference suspension of SWNTs (green diamonds, probe at 985 nm). Instrumental response function (black dots).

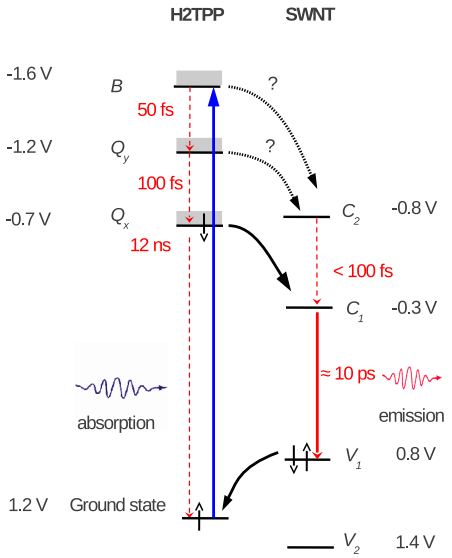

Figure 15: (color online) Scheme of the energy levels of the porphyrin molecule and of the nanotube ordered by their redox potential (vs normal hydrogen electrode). The arrows represent possible electron transfer paths. (Figure inspired from Ref. [28]).

6. Transfer mechanism

In the experimental sections, we have shown that the coupling between the H_2TPP molecules and the SWNT results in an efficient, ultrafast and temperature independent excitation energy transfer. In this section, we discuss several mechanisms that could account for these features.

First, the fact that the assembly of two species results in energy transfer rather than charge transfer is usually assessed by investigating the relative position of the energy levels of the bare species. This can be done in the present case since the measurement of the redox potentials of both H_2TPP and SWNTs have been published by several teams [38, 39, 40, 41, 42]. The energy level scheme is depicted in Fig. 15 in the particular case of (6,5) nanotubes.

Despite the substantial spread in the literature in the redox potentials of carbon nanotubes (of the order of 0.2 V), this scheme clearly shows that the H_2TPP/SWNT couple forms a type I junction leading to energy transfer, which is consistent with our observation. This is in contrast to compounds formed with other types of porphyrins or with oligomers of porphyrin that may lead to charge transfer, the nanotube being the electron acceptor [14, 16]. Previous studies of the electronic relaxation in porphyrin molecules [36] allow to build a scenario of the energy transfer subsequent to the photo-excitation of the H_2TPP molecule on the Soret transition (ground to B state transition in Fig. 15). The electron promoted in the B state rapidly relaxes down to the Q states, on a time-scale of the order of 50 fs [36]. This rapid relaxation most probably prevents the electron transfer to occur at this first stage. In contrast, the Q states have a life time of several nanoseconds which allows an electron transfer to the nanotube levels in a few hundreds of femtoseconds. In parallel, the H_2TPP ground state is repopulated on a similar time scale with an electron transfer from the valence band of the nanotube. We end up with an excited nanotube and a porphyrin molecule back in its ground state. It is hard to tell from this level scheme whether the nanotube is directly populated in its lower conduction band (C_1) or rather in its upper one (C_2). Actually, the internal conversion from C_2 to C_1 is known to occur in a few hundreds of fs [21, 37], which remains compatible with the time scale of the observed S_{11} population buildup dynamics.

The main criticism that one can oppose to this model is that it neglects the excitonic effects that are known to be central in the photo-physics of carbon nanotubes. In particular, the valence and conduction band energies are significantly renormalized in excited states and electrons and holes tends to form strongly bound pairs (excitons) [43, 44, 45], which may strongly alter the previous scheme. Another way to describe the physics of the transfer is depicted in Fig. 16. In this two-particle picture, the excitonic levels are directly excited through the desexcitation of the porphyrin molecule (through dipole-dipole interactions such as in Förster or Dexter mechanisms). This leads to the desexcitation and transfer scheme depicted in Fig. 16 and implies a resonant transfer process involving the Q states of the porphyrin and the S_{22} excitonic state of the nanotube. Although this scheme may be more satisfactory with respect to the excitonic effects, such resonant transfer effects have not been ev-

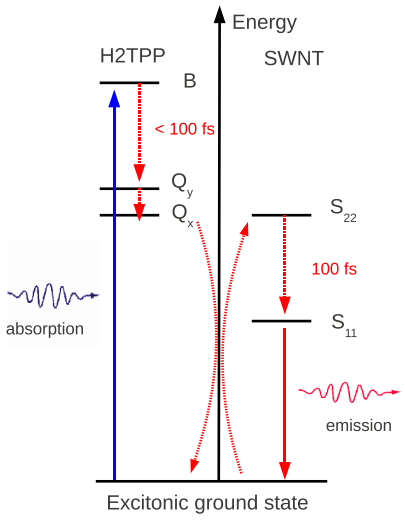

Figure 16: (color online) Scheme of the energy levels of the porphyrin molecule and of the nanotube in the excitonic picture. The arrows represent possible excitation energy transfer paths. (Figure inspired from Ref. [28]).

idenced yet. Actually, all chiral species probed in this study seem to show an extremely efficient transfer despite a sizable spread in their S_{22} energies (550-700 nm). This resonant picture may however be compatible with this spread bearing in mind the large spectral width of the Q bands (550-750 nm).

7. Conclusion

In this study we have shown that non covalently functionalized carbon nanotubes can show very promising properties that we have illustrated in the case of free base porphyrin / carbon nanotubes compounds. First, the chemical stability of the compounds can be highly enhanced using micelle assisted chemistry, which allows to obtain the formation of one single layer of porphyrin molecules wrapped on the nanotube. The suspensions show unaltered properties for months and we were also able to produce solid films which display the same functional properties. Second, the coupling between the chromophore and the nanotube can be extremely efficient despite the non-covalent binding, due to the strength of the π interactions. In the particular case of porphyrin/nanotube compounds, this results in an extremely efficient excitation energy transfer from the chromophore to the nanotube. This energy transfer allowed us to perform an all optical study of the coupling, including time-resolved studies. We have shown that the transfer occurs on a sub-picosecond time scale leading to a transfer yield as high as 99.99%. These properties are most probably not specific to the compounds based on H_2TPP but should be observable in other π stacking based compounds, opening the way to the creation of a wide class of functional materials. However, depending on the particular energy level scheme, the electronic coupling may result in other effects, such as charge transfer, an effect of utmost interest in light harvesting applications. Furthermore, the use of a cocktail of chromophores could help to cover the whole visible spectrum for improved light harvesting. On the theoretical side, the description of the electronic coupling in π stacked delocalized systems such as functionalized carbon nanotubes remains a challenge that requires further developments.

8. Methods

The details of the synthesis of the compounds are given in Ref.[24]. Absorption spectra were recorded with a Lambda 900 Perkin Elmer spectrometer. The luminescence measurements were recorded on a home-made setup based on a high power Xe lamp filtered by a monochomator. The PL signal is dispersed in a Spectrapro 2300i spectrograph and detected by an IR InGaAs photodiode array (OMAV, PI Acton). MicroPL measurements were carried out with a confocal microscope equipped with a high numerical aperture objective (Mitutoyo M Plan Apo NIR HR 100x) and recorded with a nitrogen cooled Si CCD camera. The suspension was deposited on the plane surface of a zirconium oxide solid immersion lens in order to increase PL collection. The optically detectable tube surface density was of the order of $0.1\mu m^{-2}$. For low temperature measurements, the sample was placed in a high resolution optical cryostat (Oxford Instruments Microstat HighRes2) cooled by a continuous flow of liquid helium.

Regarding time-resolved measurements, the pump-probe setup is based on an amplified Ti:sapphire laser delivering pulses at a central wavelength of 800 nm with a duration of about 130 fs and a 250 kHz repetition rate. Part of the beam is focused in a sapphire crystal to generate a white-light continuum by self-phase modulation. About 20% of this continuum is reflected off a beam splitter for use as a broad-band probe. The rest of the amplified 800 nm beam is steered into a home-made optical parametric amplifier tunable from 445 nm to 1100 nm and serves as the pump. After passing through the sample, the white probe pulse is dispersed in a spectrometer (JOBIN YVON, HR320) and is detected with a Si avalanche photodiode. We recorded the change of transmission of the sample as a function of the time delay for a given probe wavelength using standard lock-in detection techniques involving mechanical chopping of the pump beam. The chirp of the probe pulse was measured separately and is compensated in the measurements of transient spectra. The pump and probe polarizations were set at 20 degrees, but we checked that their relative orientation do not change the signal. This setup allows to cover excitation and probe wavelengths over the whole visible and NIR range with a typical 250 fs time resolution and 5 nm spectral resolution.

Appendix A. Extension of the method to other chromophores

The micelle swelling method allows to functionalize carbon nanotubes with other dye molecules such as phtalocyanine (Fig. A.17). The functionalization and the interaction between the nanotube and the molecule is evidenced by the shifts that

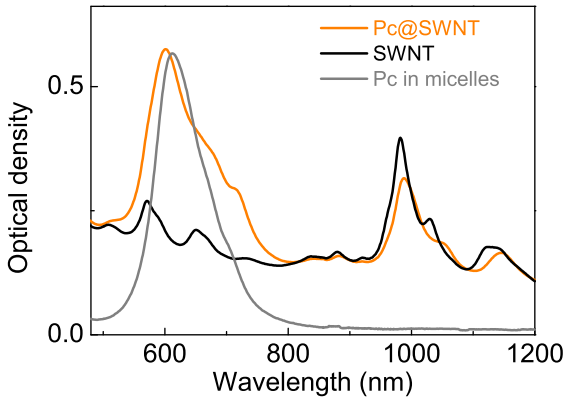

Figure A.17: (color online) Absorption spectra of micellar suspensions of phthalocyanine (grey line), SWNTs (black line) and non covalent phthalocyanine@SWNT compounds (orange line). The main absorption line of the phthalocyanine is blue shifted (11 nm) whereas the lines of SWNTs are red shifted (6 nm).

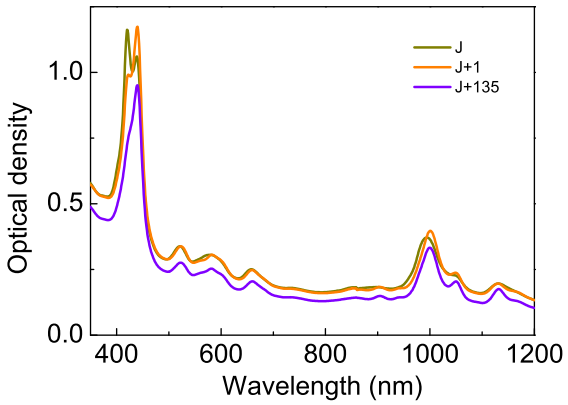

Figure B.18: (color online) Absorption spectra of H_2TPP@SWNT suspensions : as prepared (green line), after 1 day (orange line) and after 4.5 months. The maturation process leads to an increased functionalization and a decrease of the scattering background.

can be oberved both for the dye and the nanotube lines. The nanotube S_{11} line experiences a red shift as in the case of porphyrins. In contrast, the bands of the phthalocyanine are blue shifted. This may be related to a specific conformational change of the molecule to accomodate the nanotube shape. Finally, note that these compounds do not lead to any detectable energy transfer.

Appendix B. Stability of the compounds

We investigated the chemical stability of the material. Fig. B.18 shows the absorption spectra of an as-prepared suspension together with the spectra of the same suspension recorded one day and four months later. The spectra are essentially similar, which shows the excellent stability of the suspension. In addition, a slight change in the Soret band shows that the maturation process that occurs in the dynamical equilibrium of micellar suspensions tends to increase the functionalization degree with a sizable increase of the Soret band at 440 nm at the expense of the free H_2TPP line at 420 nm. This shows that the functionalized tubes are more stable than the bare components (H_2TPP and SWNTs) separately inserted in micelles.

Appendix C. Solid films

Moreover, we were able to produce thin solid films of this material by simply drying a drop of the suspension on a quartz substrate, or by filtration of the suspension through a 0.2 μm porous nitrocelluloid filter and further dissolution in acetonitrile. The absorption spectrum of the material is not significantly modified as compared to the suspension (Fig. C.19) except for a slight broadening of the lines. Furthermore, the films show a large NIR photoluminescence signal and a good photo-stability (Fig. C.20). Finally, the energy transfer properties of the H_2TPP@SWNTs compounds are preserved when condensed into a solid film.

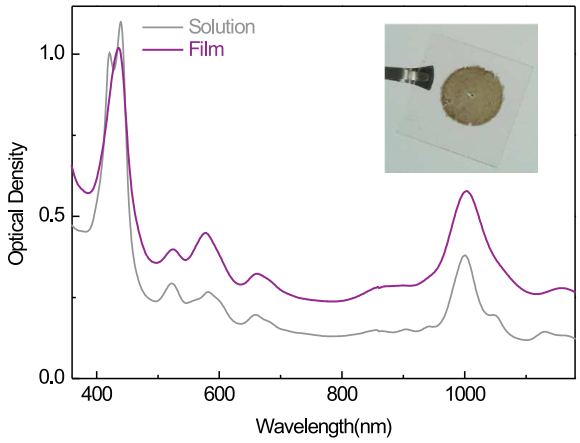

Figure C.19: (color online) Absorption spectrum of a film of H_2TPP@SWNT together with the absorption spectrum of the suspension used to make it. Inset : picture of the film deposited on a quartz substrate.

[1] J. Lefebvre, Y. Homma, P. Finnie, Bright band gap photoluminescence from unprocessed single-walled carbon nanotubes, Phys. Rev. Lett. 90 (2003) 217401.

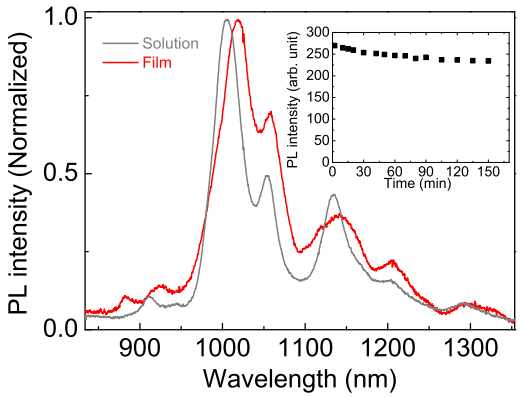

Figure C.20: (color online) PL spectrum of a film of H_2TPP@SWNT (excitation : 532 nm, power : 0.4 kW/cm^2) together with the PL spectrum of the suspension used to make it. Inset : PL intensity of the film as a function of exposure time, showing the good photo-stability.

[2] S. Berger, F. Iglesias, P. Bonnet, C. Voisin, G. Cassabois, J. S. Lauret, C. Delalande, P. Roussignol, Optical properties of carbon nanotubes in a composite material: The role of dielectric screening and thermal expansion, Journal of Applied Physics 105 (2009) 094323.

[3] Y.-M. Lin, J. C. Tsang, M. Freitag, P. Avouris, Impact of oxide substrate on electrical and optical properties of carbon nanotube devices, Nanotechnology 18 (2007) 295202–.

[4] B. Chandra, V. Perebeinos, S. Berciaud, J. Katoch, M. Ishigami, P. Kim, T. F. Heinz, J. Hone, Low bias electron scattering in structure-identified single wall carbon nanotubes: Role of substrate polar phonons, Phys. Rev. Lett. 107 (2011) 146601–.

[5] M. J. O'Connell, S. M. Bachilo, C. B. Huffman, V. C. Moore, M. S. Strano, E. H. Haroz, K. L. Rialon, P. J. Boul, W. H. Noon, C. Kittrell, J. Ma, R. H. Hauge, R. B. Weisman, R. E. Smalley, Band gap fluorescence from individual single-walled carbon nanotubes, Science 297 (2002) 593–596.

[6] J. S. Lauret, C. Voisin, G. Cassabois, P. Roussignol, C. Delalande, A. Filoramo, L. Capes, E. Valentin, O. Jost, Bandgap photoluminescence of semiconducting single-wall carbon nanotubes, Physica E-Low-Dimensional Systems and Nanostructures 21 (2004) 1057–1060. 11th International Conference on Modulated Semiconductor Structures (MSS11), Nara, Japan, 2003.

[7] W. Walden-Newman, I. Sarpkaya, S. Strauf, Quantum light signatures and nanosecond spectral diffusion from cavity-embedded carbon nanotubes, Nano Lett. 12 (2012) 1934–1941.

[8] S. Moritsubo, T. Murai, T. Shimada, Y. Murakami, S. Chiashi, S. Maruyama, Y. K. Kato, Exciton diffusion in air-suspended single-walled carbon nanotubes, Phys. Rev. Lett. 104 (2010) 247402.

[9] Z. Liu, S. Tabakman, K. Welsher, H. Dai, Carbon nanotubes in biology and medicine: In vitro and in vivo detection, imaging and drug delivery, Nano Research 2 (2009) 85–120. 10.1007/s12274-009-9009-8.

[10] B. J. Landi, R. P. Raffaelle, S. L. Castro, S. G. Bailey, Single-wall carbon nanotube¢polymer solar cells, Progress in Photovoltaics: Research and Applications 13 (2005) 165–172.

[11] L. Cognet, D. A. Tsyboulski, J.-D. R. Rocha, C. D. Doyle, J. M. Tour, R. B. Weisman, Stepwise quenching of exciton fluorescence in carbon nanotubes by single-molecule reactions, Science 316 (2007) 1465–1468.

[12] C. A. Dyke, J. M. Tour, Covalent functionalization of single-walled carbon nanotubes for materials applications, J. Phys. Chem. A 108 (2004) 11151–11159.

[13] S. D. Stranks, C. Weisspfennig, P. Parkinson, M. B. Johnston, L. M. Herz, R. J. Nicholas, Ultrafast charge separation at a polymer-single-walled carbon nanotube molecular junction, Nano Letters 11 (2011) 66–72.

[14] S. D. Stranks, J. K. Sprafke, H. L. Anderson, R. J. Nicholas, Electronic and mechanical modification of single-walled carbon nanotubes by binding to porphyrin oligomers, ACS Nano 5 (2011) 2307–2315.

[15] V. Sgobba, D. M. Guldi, Carbon nanotubes-electronic/electrochemical properties and application for nanoelectronics and photonics, Chem. Soc. Rev. 38 (2009) 165.

[16] D. M. Guldi, H. Taieb, G. M. A. Rahman, N. Tagmatarchis, M. Prato, Novel photoactive single-walled carbon nanotube-porphyrin polymer wraps: Efficient and long-lived intracomplex charge separation, Advanced Materials 17 (2005) 871–875.

[17] G. M. A. Rahman, D. M. Guldi, S. Campidelli, M. Prato, Electronically interacting single wall carbon nanotube-porphyrin nanohybrids, Journal Of Materials Chemistry 16 (2006) 62–65.

[18] W. M. Campbell, K. W. Jolley, P. Wagner, K. Wagner, P. J. Walsh, K. C. Gordon, L. Schmidt-Mende, M. K. Nazeeruddin, Q. Wang, M. Graetzel, D. L. Officer, Highly efficient porphyrin sensitizers for dye-sensitized solar cells, The Journal of Physical Chemistry C 111 (2007) 11760–11762.

[19] P. H. Tan, A. G. Rozhin, T. Hasan, P. Hu, V. Scardaci, W. I. Milne, A. C. Ferrari, Photoluminescence spectroscopy of carbon nanotube bundles: Evidence for exciton energy transfer, Phys. Rev. Lett. 99 (2007) 137402.

[20] O. N. Torrens, D. E. Milkie, M. Zheng, J. M. Kikkawa, Photoluminescence from intertube carrier migration in single-walled carbon nanotube bundles, Nano Letters 6 (2006) 2864–2867.

[21] J. S. Lauret, C. Voisin, G. Cassabois, C. Delalande, P. Roussignol, O. Jost, L. Capes, Ultrafast carrier dynamics in single-wall carbon nanotubes, Physical Review Letters 90 (2003) 057404.

[22] G. Magadur, J.-S. Lauret, V. Alain-Rizzo, C. Voisin, P. Roussignol, E. Deleporte, J. A. Delaire, Excitation transfer in functionalized carbon nanotubes, ChemPhysChem 9 (2008) 1250–1253.

[23] F. Ernst, T. Heek, A. Setaro, R. Haag, S. Reich, Energy transfer in nanotube-perylene complexes, Advanced Functional Materials (2012).

[24] C. Roquelet, J.-S. Lauret, V. Alain-Rizzo, C. Voisin, R. Fleurier, M. Delarue, D. Garrot, A. Loiseau, P. Roussignol, J. A. Delaire, E. Deleporte, Pi-stacking functionalization of carbon nanotubes through micelle swelling, ChemPhysChem 11 (2010) 1667–1672.

[25] R. K. Wang, W.-C. Chen, D. K. Campos, K. J. Ziegler, Swelling the micelle core surrounding single-walled carbon nanotubes with water-immiscible organic solvents, J. Am. Chem. Soc. 130 (2008) 16330–16337.

[26] W.-C. Chen, R. K. Wang, K. J. Ziegler, Coating individual single-walled carbon nanotubes with nylon 6,10 through emulsion polymerization, ACS Appl. Mater. Interfaces 1 (2009) 1821–1826.

[27] G. Clave, G. Delport, C. Roquelet, J.-S. Lauret, E. Deleporte, F. Vialla, B. Langlois, R. Parret, C. Voisin, P. Roussignol, B. Jousselme, P. Jegou, A. Gloter, O. Stephan, A. Filoramo, V. Derycke, S. Campidelli, Functionalization of carbon nanotubes through polymerisation in micelles: a bridge between the covalent and noncovalent methods., (submitted) (2012).

[28] D. Garrot, B. Langlois, C. Roquelet, T. Michel, P. Roussignol, C. Delalande, E. Deleporte, J.-S. Lauret, C. Voisin, Time-resolved investigation of excitation energy transfer in carbon nanotube-porphyrin compounds, J. Phys. Chem. C 115 (2011) 23283–23292.

[29] C. Roquelet, D. Garrot, J. S. Lauret, C. Voisin, V. Alain-Rizzo, P. Roussignol, J. A. Delaire, E. Deleporte, Quantum efficiency of energy transfer in noncovalent carbon nanotube/porphyrin compounds, Applied Physics Letters 97 (2010) 141918.

[30] S. Berciaud, L. Cognet, B. Lounis, Luminescence decay and the absorption cross section of individual single-walled carbon nanotubes, Physical Review Letters 101 (2008) 077402.

[31] J. B. Kim, J. J. Leonard, F. R. Longo, Mechanistic study of the synthesis and spectral properties of meso-tetraarylporphyrins, J. Am. Chem. Soc. 94 (1972) 3986–3992.

[32] J. Lefebvre, P. Finnie, Excited excitonic states in single-walled carbon nanotubes, Nano Letters 8 (2008) 1890–1895.

[33] T. Hasobe, S. Fukuzumi, P. V. Kamat, Ordered assembly of protonated porphyrin driven by single-wall carbon nanotubes. j- and h-aggregates to nanorods, J. Am. Chem. Soc. 127 (2005) 11884–11885.

[34] D. A. Tsyboulski, J.-D. R. Rocha, S. M. Bachilo, L. Cognet, R. B. Weisman, Structure-dependent fluorescence efficiencies of individual single-walled carbon nanotubes, Nano Letters 7 (2007) 3080–3085.

[35] S. Reich, C. Thomsen, J. Robertson, Exciton resonances quench the pho-

toluminescence of zigzag carbon nanotubes, Phys. Rev. Lett. 95 (2005) 077402.
[36] J. S. Baskin, H. Z. Yu, A. H. Zewail, Ultrafast dynamics of porphyrins in the condensed phase: I. free base tetraphenylporphyrin, Journal of Physical Chemistry A 106 (2002) 9837–9844.
[37] C. Manzoni, A. Gambetta, E. Menna, M. Meneghetti, G. Lanzani, G. Cerullo, Intersubband exciton relaxation dynamics in single-walled carbon nanotubes, Phys. Rev. Lett. 94 (2005) 207401.
[38] J. P. Casey, S. M. Bachilo, R. B. Weisman, Efficient photosensitized energy transfer and near-ir fluorescence from porphyrin-swnt complexes, J. Mater. Chem. 18 (2008) 1510–1516.
[39] Y. Tanaka, Y. Hirana, Y. Niidome, K. Kato, S. Saito, N. Nakashima, Experimentally determined redox potentials of individual (n,m)single-walled carbon nanotubes, Angewandte Chemie International Edition 48 (2009) 7655–7659.
[40] A. Nish, R. J. Nicholas, Temperature induced restoration of fluorescence from oxidised single- walled carbon nanotubes in aqueous sodium dodecylsulfate solution, Phys Chem Chem Phys 8 (2006) 3547.
[41] M. Zheng, B. A. Diner, Solution redox chemistry of carbon nanotubes, Journal of the American Chemical Society 126 (2004) 15490–15494.
[42] D. Paolucci, M. M. Franco, M. Iurlo, M. Marcaccio, M. Prato, F. Zerbetto, A. Penicaud, F. Paolucci, Singling out the electrochemistry of individual single-walled carbon nanotubes in solution, Journal of the American Chemical Society 130 (2008) 7393–7399.
[43] T. Ando, Excitons in carbon nanotubes, Journal of the Physical Society of Japan 66 (1997) 1066–1073.
[44] F. Wang, G. Dukovic, L. E. Brus, T. F. Heinz, The optical resonances in carbon nanotubes arise from excitons, Science 308 (2005) 838–841.
[45] J. Maultzsch, R. Pomraenke, S. Reich, E. Chang, D. Prezzi, A. Ruini, E. Molinari, M. S. Strano, C. Thomsen, C. Lienau, Exciton binding energies in carbon nanotubes from two-photon photoluminescence, Phys. Rev. B 72 (2005) 241402.